Published in final edited form as:
J Comp Neurol. 2012 May 1; 520(7): 1365–1375. doi:10.1002/cne.22797.

Planar Multipolar Cells in the Cochlear Nucleus Project to Medial Olivocochlear Neurons in Mouse

Keith N. Darrow[1,2], **Thane E. Benson**[2], and **M. Christian Brown**[2,3]

[1]Department of Communication Sciences and Disorders, Worcester State University

[2]Eaton-Peabody Laboratory, Massachusetts Eye and Ear Infirmary

[3]Department of Otology and Laryngology, Harvard Medical School, Boston, MA 02114, USA

Abstract

Medial olivocochlear (MOC) neurons originate in the superior olivary complex and project to the cochlea, where they act to reduce the effects of noise masking and protect the cochlea from damage. MOC neurons respond to sound via a reflex pathway, however, in this pathway the cochlear nucleus cell type that provides input to MOC neurons is not known. We investigated whether multipolar cells of the ventral cochlear nucleus have projections to MOC neurons, by labeling them with injections into the dorsal cochlear nucleus. The projections of one type of labeled multipolar cell, planar neurons, were traced into the ventral nucleus of the trapezoid body, where they were observed terminating on MOC neurons (labeled in some cases by a second cochlear injection of Fluorogold). These terminations formed what appear to be excitatory synapses, i.e. containing small, round vesicles and prominent postsynaptic densities. These data suggest that cochlear nucleus planar multipolar neurons drive the MOC neuron's response to sound.

Indexing Terms

synapse; reflex; superior olivary complex; descending system

INTRODUCTION

Medial olivocochlear (MOC) neurons originate in the superior olivary complex (SOC) and project to the cochlea (Fig. 1). These neurons respond to sound as part of the MOC reflex, which plays an important role in reducing the effects of background noise and in protecting the cochlea from acoustic overexposure (rev. by (Ryugo et al., 2011). The response to sound is mediated by a neural pathway consisting of three stages (Fig. 1). The first stage consists of auditory nerve fibers, which receive synapses from cochlear hair cells and convey sound-evoked discharges to the brainstem. The intermediate, and least understood, stage consists of cochlear nucleus (CN) neurons located in the posteroventral (PVCN) subdivision (Warr, 1969; Thompson and Thompson, 1991a; de Venecia et al., 2005), which respond to auditory-nerve inputs and project to the MOC neurons. The third, or efferent, stage is composed of MOC neurons, which project back to the cochlea and exert their inhibitory synaptic effects on outer hair cells.

Correspondence to: Keith N. Darrow, Worcester State University, Department of Communication Sciences and Disorders, Worcester, MA, 01564, USA. Phone: 508-929-8551. Fax: 508-929-8175. Kdarrow@worcester.edu.

The focus of this study is to determine the CN neurons involved in the intermediate stage of the MOC reflex. Although this stage involves the PVCN, the precise neurons have not been identified. Multipolar cells are leading candidates, because their sound-evoked responses, as those of the MOC neurons, do not adapt (Brown et al., 2003; de Venecia et al., 2005). However, multipolar cells are a heterogeneous group, with several subtypes each having different responses and projections (Rhode and Smith, 1986; Oertel et al., 2011). Their projections are difficult to study. Multipolar somata are intermixed with other cell types in the CN, which makes it hard to selectively label them. Their axons, at least those that project ventrally toward the SOC, are thin and difficult to impale, which makes them hard to label with sharp electrodes.

In the current study, we selectively label multipolar cells via their collaterals to the dorsal cochlear nucleus (DCN) (Ostapoff et al., 1999; Doucet and Ryugo, 2003, 2006). Of the many types of VCN cells, only multipolar cells send collaterals to the DCN (Adams, 1983). Thus, injection of neuronal tracer into the DCN allows us to selectively examine multipolar cell projections without contamination from other labeled axons from the VCN. We then used electron microscopy to determine which of the known classes of synaptic terminal types identified in prior studies (White, 1984; Spangler et al., 1986; Helfert et al., 1988; Benson and Brown, 2006) originate from multipolar cell inputs.

MATERIALS AND METHODS

All experimental procedures on CBA/CaJ mice were performed in accordance with the National Institutes of Health guidelines for the care and use of laboratory animals as well as approved animal care and use protocols at the Massachusetts Eye & Ear Infirmary. Mice were aged 8 – 12 weeks, weighing 20 – 26 g., and of either sex. Following anesthesia (xylazine 20 mg/kg i.p. and ketamine 100 mg/kg i.p.) the mouse was held in a Kopf small-animal stereotaxic apparatus by snout clamp and ear bars. The skin overlaying the skull was slit and a craniotomy of the left posterior skull surface was performed using rongeurs. Partial cerebellar aspiration (of the left hemisphere) exposed the dorsal surface of the brainstem. The surface landmarks and the ampulla of the superior semicircular canal were used to identify the DCN.

Thirty-two mice had single injections into the DCN and 11 of these were studied in detail. The DCN injections were made using a broken-tip micropipette hermetically coupled to a 1.0 ml Hamilton syringe. The pipette was filled with the anterograde tracer biotinylated dextran-amine (BDA) (MW 10,000, Molecular Probes) as a 10% solution in 0.01 M phosphate buffer. Current (+ 5 mA in pulses of 7 s on, 7 s off) was applied to the exposed needle of the Hamilton syringe for 8–12 min. Immediately following injection, the incision was closed and the scalp was sutured. After a 4–5 day survival time, the animals for study with the light microscope were perfused intracardially with physiologic saline followed by 4% paraformaldehyde in 0.05 M phosphate buffer (pH 7.2). The brainstems were extracted, post-fixed 2 hours, cryoprotected in 30% sucrose overnight, frozen and cut on a sliding microtome at 80 μm in the transverse plane. Free-floating sections for the single-injection cases were treated with 0.5% hydrogen peroxide, washed in phosphate buffer and incubated in ABC (Vector Labs Vectastain ABC kit PK 4000) overnight at room temperature. Color development was achieved with DAB, 1% nickel ammonium sulfate, and 1% cobalt chloride. Only the cases with the injection site restricted to the DCN were analyzed for the purpose of this study (in the cases that the injection encroached upon the VCN thick axons crossing the trapezoid body were observed).

Ten additional mice received DCN injections and also received a second injection into the ipsilateral cochlea (re: DCN, Fig. 1) of Fluorogold (Fluorochrome LLC), which was used to

retrogradely label olivocochlear neurons (Brown and Levine, 2008). Five of these double-injection cases had DCN injections of DA that was conjugated with Alexa Fluor 568 (Invitrogen), in which case they were examined in the fluorescent microscope without further processing. The fluorescent tissue was photographed with a 10x objective and overlaid images of the FG and DA markers were used to estimate the number of synaptic contacts (contacts were counted only if there were in the same focal plane as the labeled neuron's soma or dendrite). The remaining five mice had DCN injections of BDA, in which case they were processed using an anti-Fluorgold antibody (Fluorochrome LLC) (Brown and Levine, 2008) and the BDA processing describe above. In this material, the MOC neurons are labeled a brown color and the BDA labeled terminals are black. In these cases, counts of synaptic contacts were make using a 40x objective.

Two additional mice were processed for electron microscopy and each received a single injection of BDA into the DCN. These mice were perfused with physiologic saline followed by 0.5% paraformaldehyde and 1% glutaraldehyde in 0.1 M cacodylate buffer (pH 7.3). This was followed by 0.5% paraformaldehyde and 3% glutaraldehyde in buffer. After an hour in the skull, the brainstems were removed and fixed an additional hour before immersion in cacodylate-buffered saline overnight. The brainstems were then embedded in gelatin-albumin, sectioned with a vibratome (80 μm), and processed for BDA as above. Select sections were stained with 1% OsO_4, and then 1% uranyl acetate. The sections were dehydrated with methanol, infiltrated with epoxy, and flat-embedded between two transparent sheets of Aclar (Pro Plastics, Wall, NJ).

Fiber diameters were measured by tracing the outline of the labeled fiber using a light microscope equipped with a drawing tube. Using ImageJ, we measured the area of the fiber and divided it by the path length (over a length about 100 μm) to obtain the average diameter. The reconstruction of Figure 6A used a 40x objective to take a fiber-following focus sequence of digital micrographs without moving the specimen stage. The in-register files were entered as 18 layers in Photoshop with a drawing layer of 50% opacity. A Wacom tablet and stylus were used to trace in-focus portions of the labeled fiber, neurons, etc., from each layer. When the drawing was complete, it was verified in the microscope and the focus micrometer was used to determine the z (μm depth) of different portions of the fiber and other structures. One layer was chosen as a background.

Electron micrographs (800 to 25,000x) were captured using a digital camera (Model 15C Scientific Instruments and Applications, Inc., Duluth GA) in 16 bit .tiff format. The micrographs were processed using only the Levels function of Adobe Photoshop CS. Morphometric data on synaptic vesicles (Fig. 6E) were obtained from images of 25,000x original magnification (similar to Fig. 6C). In sections containing the synapse, the vesicles close to the synaptic specializations were traced along the outer edges of their membranes using a digitizing tablet. Vesicle area and circularity ($4\pi(\text{area}/\text{perimeter}^2)$) were computed using ImageJ by measuring 11–40 vesicles that were in the terminal. Maximal distance from the specialization ranged from 250 – 800 nm in order to acquire a sufficient number of vesicles to accurately estimate mean area and circularity. Vesicles were measured in up to 2 sections per synapse. Within a single terminal, the vesicles measurements were combined to form a per-terminal mean area and mean circularity (Fig. 6E). T-tests were considered significant for $p<0.05$.

RESULTS

Labeled cell bodies in cochlear nucleus and axonal projections

After injections of the anterograde tracer, biotinylated dextran amine (BDA), into the DCN, there are labeled neurons and fibers in the VCN (Fig. 2). The labeled neurons that are dark

enough to be classified are either multipolar cells (Hackney et al., 1990), having 3–5 dendrites per cell, or small cells (10 μm diam.) and granule cells. The small cells are found near the edges of the VCN and, since their axons could not be followed, they will not be considered further. Neither bushy cells nor octopus cells are labeled in our material in which the injection sites are confined to the DCN.

Most of the labeled multipolar cells are “planar” neurons (Doucet and Ryugo, 1997; Doucet et al., 1999; Doucet and Ryugo, 2006) and are organized in a band within the VCN (Fig. 3). Their somata are of medium size (20 μm diam.). Their dendrites are difficult to separate from the accompanying labeled fibers (Fig. 3A). These fibers are mostly auditory nerve branches that arise from labeled parent axons in the auditory nerve. Some of them may be from DCN neurons such as vertical cells (Wickesberg and Oertel, 1990). A few “radiate” multipolar cells (Doucet et al., 1999) are labeled outside the band of planar neurons. They have larger somata (25 μm diam.) and thick, well-labeled dendrites that radiate in all directions with extensive courses through the CN.

Axons (red lines in Fig. 3B) project out of the labeled band ventromedially toward the ventral acoustic stria. We will assume these axons are from planar multipolar neurons because almost all the labeled neurons in the band are of this type. Also, the axons appear to be from a single population in terms of their appearance and diameter. The axonal diameters near the midline averaged 1.40 μm (for 10 fibers) which were slightly, but significantly, smaller than auditory nerve fibers (avg. 1.64 μm for 10 fibers, P=.005) measured in the nerve stump and labeled by the same injections. Along their course, the planar neuron axons have constrictions that we interpret as nodes of Ranvier (Liberman and Oliver, 1984), thus the fibers are likely to be myelinated. In the electron microscope, we confirmed this myelination (Fig. 5A).

Each injection also labeled fibers that project out the dorsal acoustic stria (not illustrated). This group of fibers crosses the midline in the dorsal half of the brainstem and eventually runs in the lateral lemniscus to inntervate the contralateral inferior colliculus. A few fibers in this group, however, innervate the CN on the opposite side (Brown et al., 2012). Some of the large DCN injections also produce a few retrogradely labeled somata in the ipsilateral LNTB and peri-LSO region, and more rarely, in the contralateral CN.

Labeled branches in the superior olivary complex

Labeled fibers enter the SOC and produce branches to two main nuclei: the ipsilateral lateral superior olive (LSO) and the contralateral ventral nucleus of the trapezoid body (VNTB; Figs. 1, 4). For a total of 12 axons reconstructed from the edge of the CN to the contralateral lateral lemniscus, all form at least one branch to the SOC, 10 (83%) form branches to the ipsilateral LSO, 6 (50%) form branches to the contralateral VNTB. Of the 12 axons, 4 (33%) branch to both ipsilateral LSO and contralateral VNTB. Many other fibers were traced whose complete course could not be reconstructed because of fading or intermingling; a few of these form branches to the ipslateral VNTB. We did not observe any labeled branches to the contralateral LSO. For the two axons of Figure 4, the average distance from fiber origin in the VCN to branch termination in the contralateral VNTB is 4.6 mm. After passing the SOC, the axons coalesce in the lateral lemniscus to course toward the inferior colliculus.

The labeled branches to the VNTB are very fine in caliber (diam. about 0.5 μm). This estimate from the light microscope is confirmed by electron microscopic images (Fig. 5B). These images also show that the branches are unmyelinated, at least in the region where they form swellings (Fig. 5B). They produce en passant and terminal swellings that are mostly round in shape and usually small in diameter (< 3 μm). These characteristics are almost identical to those of swellings in the ipsilateral LSO, but the VNTB branches are shorter and

produce fewer swellings per branch. The number of swellings was documented for VNTB branches that could be followed to all their endings (e.g., Fig. 6A). The 2 ipsilateral and 6 contralateral VNTB branches contained an average of 19.9 en passant swellings (range 11–31) and 6.9 terminal swellings (range 3 – 16).

The topography of VNTB branches differs from that of LSO branches. LSO branches emanate in a dorsal direction and terminate in one segment of the LSO, and the segment is narrow along the LSO's tonotopic organization from lateral to medial (Doucet and Ryugo, 2003). Because of this dense termination of many branches labeled by a single injection, and because the LSO branches have many sub-branches, it was not possible to reconstruct any of them individually. In contrast to LSO branches, VNTB branches from one injection are spatially separate (Fig. 4). Their orientations are diverse with some running dorso-ventrally (Fig. 4) and others running medio-laterally (Fig. 6A). None of them, however, run rostro-caudally and each branch's extent in that direction was contained within one or two 80 μm thick sections. The branch illustrated in Figure 6A had a rostro-caudal extent of only 16 μm.

Double Injections

To determine whether OC neurons are targeted by neurons labeled by the DCN injections, OC neurons were retrogradely labeled by a cochlear injection of the retrograde tracer Fluorogold (FG) on the same side as the DCN injection (Fig. 1). Most labeled OC neurons were located in the VNTB contralateral to the injected cochlea, thus identifying them as part of the medial (M)OC system projecting to OHCs (Campbell and Henson, 1988; Brown and Levine, 2008). These FG-labeled neurons are contacted by terminals labeled by the DCN injections. Figure 7 is an example in which the terminals that are labeled with fluorescently tagged DA (red) contacted FG-labeled MOC neurons (blue) in the VNTB contralateral to the injected cochlea. The contacts are observed on the MOC neuron somata and dendrites (Fig. 7, arrowheads vs. arrows). In double-injected cases, we counted a total of 89 MOC neurons that received DA-labeled terminals in the contralateral VNTB (n=5 cases) and an additional 64 that contacted MOC neurons in the ipsilateral VNTB (n=4 cases). In 5 additional cases, BDA was injected in the DCN. This material yielded an additional 62 MOC neurons that were contacted in the contralateral VNTB and 35 in the ipsilateral VNTB.

Synapses formed by labeled branches in contralateral VNTB

To investigate synapses and targets of BDA-labeled axons, two branches within the contralateral VNTB were examined in the electron microscope. The material is from two animals in which single injections of BDA were made into the DCN. Labeled branches give rise to synapses (denoted by arrowheads on Figs. 6, 8) that contain post-junctional dense material (thus having an asymmetric appearance), clear synaptic vesicles, and a cleft of uniform thickness. Of the 19 synapses, two contained dense-core vesicles (Fig. 6D). The synapses are formed by swellings of the labeled branches, although one swelling examined in complete serial sections did not form any identifiable synapses (Fig. 5B). Single terminals can form multiple synapses. For example, the swelling illustrated in Figure 6A (arrow), for which serial sections were available only for part of its extent, forms a total of 5 synapses (one illustrated in Fig. 6C).

Three types of terminals were previously described on MOC neurons (White, 1984; Spangler et al., 1986; Helfert et al., 1988; Benson and Brown, 2006). Our results suggest that those from planar neurons have small, round synaptic vesicles. Measurements of synaptic vesicles were made from 3 labeled terminals (e.g., Fig. 6C) from different swellings of the branch illustrated in Figure 6A. Mean vesicle areas range from 521 to 634 nm^2, and mean coefficients of circularity range from 0.89 to 0.93 (filled circles in Figure 6E). Among unlabeled terminals (Fig. 6E, unfilled circles), six have the same type of "small, round"

vesicles as the labeled terminals. Two of the unlabeled terminals have vesicles with larger areas ("large, round"), and another two have vesicles with lower circularities ("pleomorphic").

Synaptic targets

The postsynaptic target of 5 synapses from one of the branches examined is a neural soma (N in Fig. 6A, B). This neuron is 12.5 μm × 25 μm in size. The soma is contacted by only a few other unlabeled terminals (Fig. 6D, 12% coverage of the somatic membrane as measured in one section that contains the nucleus). The labeled branch also forms two contacts on a smaller neuron (about 6 μm diam., not illustrated), but both of these contacts are non-synaptic.

For the remainder of the synapses (14/19), the targets are dendrites (Fig. 8). These dendrites are of various morphology, but are usually small (< 1 μm diam.). They are among many other dendrites found in the VNTB in islands of neuropil that lie among the axons of passage. One target dendrite, indicated in two segments in the center of Figure 8A, receives 6 synapses along its course. In another instance, there is a labeled synapse on a dendritic spine (sp, Fig. 8D). In two additional instances, target dendrites intervened between the labeled terminals and cell bodies (e.g., N in Fig. 8B). The cell bodies had been interpreted as the post-synaptic target in the light microscope, but instead the synaptic targets are the intervening dendrites.

DISCUSSION

Neurons Labeled by DCN Injections

In this study, labeled axons were traced from the VCN to the superior olivary complex, where they formed branches that terminated on MOC neurons. Planar neurons are the presumed source of this projection as they constitute the vast majority of VCN labeled neurons resulting from the type of DCN injections that were made. Planar neurons are a major subtype of multipolar cell that were originally distinguished by Doucet and Ryugo (1997). They almost certainly correspond to earlier-defined subtypes known as "T-stellate cells" (Doucet and Ryugo, 2006; Oertel et al., 2011) and/or "type I stellate cells" (Cant, 1981). Other, less numerous multipolar cells labeled by DCN injections include radiate neurons. They are unlikely to contribute to the projections we studied because their axons project dorsally, most likely to cross the brainstem and terminate in the contralateral CN (Doucet and Ryugo, 2006; Brown et al., 2012). Radiate neurons may correspond to "D-stellate cells" and "type II stellate cells" (Doucet and Ryugo, 2006; Oertel et al., 2011). Smaller neurons along the margins of the VCN are also labeled, however, it is not clear whether these neurons contribute to our labeled projections. We were not able to follow their axons, which are expected to be thin in diameter. Overall, the pattern of cell labeling in mice replicates that seen by Doucet and Ryugo (2006) in rats.

DCN injections also label axons of presumed pyramidal and giant cells, which project out the dorsal acoustic stria and cross the brainstem. Some of them give off branches to the contralateral SOC, but they are thicker, form bigger endings, and terminate in positions caudal to the MOC neurons. As branches from dorsal acoustic stria axons have not been reported previously (Thompson and Thompson, 1991a); they may be unique to mice. DCN injections also label a few neurons in the periolivary nuclei associated with the ipsilateral LSO (Adams and Warr, 1976). This labeling was potentially a contaminating factor in our double injected cases, because there are a few presumed MOC neurons associated with the LSO in mouse (Brown and Levine, 2008). Our labeling methods colored the retrogradely labeled MOC neurons differently than the anterogradely labeled branches (e.g., Fig. 7), and

we confined our observations to the VNTB so as to avoid confusion with neurons whose origins are potentially ambiguous.

Projections to MOC Neurons

Our study of projections to MOC neurons builds on earlier work that showed PVCN projections to the periolivary regions (Warr, 1969) and to the OC neurons (Thompson and Thompson, 1991b). Many planar neurons are located in PVCN (e.g., Fig. 3) (Doucet and Ryugo, 1997), and PVCN lesions have been demonstrated to interrupt the sound-evoked MOC reflex (de Venecia et al., 2005). In the present study, the most common projection was to MOC neurons on the opposite side of the brain, which in turn project back across the midline to the ipsilateral cochlea (Fig. 1). A smaller number of projections are to ipsilateral MOC neurons. One difference between our work in mice and that in guinea pig (Thompson and Thompson, 1991a) is the location of the MOC neurons within the olivary complex. In mice, they are located mainly in the VNTB, whereas in the guinea pig, they have a more widespread distribution that also includes the superior paraolivary nucleus and the medial nucleus of the trapezoid body (Thompson and Thompson, 1991a; Aschoff and Ostwald, 1988). In addition, the mouse has higher percentage of MOC neurons on the contralateral side (about 75%; Campbell and Henson, 1988) compared to other species.

In our material, as in earlier studies (Doucet and Ryugo, 2003), the axons of planar neurons project to the ipsilateral LSO and to the contralateral VNTB. The terminations that are formed in these two nuclei are similar: very thin branches that form small en passant and terminal swellings. In the ipsilateral LSO, the branches terminate in a narrow strip related tonontopically to the injection site (Doucet and Ryugo, 2003). In the contralateral VNTB, the branches terminate in a less organized pattern but the extent of each branch is narrow in the rostro-caudal direction. Whether the branches or the VNTB neurons themselves have a tonotopic organization in this direction or any other is not clear, but the fact that the VNTB has a long axis in the rostro-caudal dimension is suggestive (Campbell and Henson, 1988; Darrow et al., 2007; Brown and Levine, 2008). Some of the labeled branches we studied are oriented medio-laterally (Fig. 6A), which is the direction in which MOC neurons have their longest dendrites (Brown and Levine, 2008). However, descending projections from the tonotopically organized central nucleus of the inferior colliculus suggest a lateral to medial tonotopic organization of the VNTB (Caicedo and Hervert, 1993). Further work is needed to clarify the organization of the VNTB.

Synapses of Multipolar Cells

The synaptic terminals from planar neuron branches have small, round vesicles and form asymmetric synapses. While our study did not directly show planar neuron synapses on MOC neurons, this type of synapse has been reported on all previous studies of MOC ultrastructure (White, 1984; Spangler et al., 1986; Helfert et al., 1988; Benson and Brown, 2006). Our synapses have other features reported previously: some terminals contain dense-core vesicles, and the terminals themselves are of moderate size, smaller than terminals with large, round vesicles. Single terminals can form multiple synapses onto a given target (Fig. 8), suggesting a strong postsynaptic effect (Benson and Brown, 2006). One of the targets of the present study was a soma with characteristics consistent with MOC neurons: it is in the size range for MOC neurons in mice (Brown and Levine, 2008) and its soma had only 12% coverage by terminals (Benson and Brown, 2006). In the light microscope, we observed contacts between MOC somata and dendrites (Fig. 6), but our ultrastructural observations (Fig. 8) suggest that some of these putative somatic contacts may actually be forming synapses on intervening dendrites. One of the targets was a dendritic spine and MOC dendrites are known to have spines (Mulders and Robertson, 2000). The synaptic morphology we describe is also consistent with previous studies of multipolar collaterals in

VCN (Smith et al., 1993) and their terminations in inferior colliculus (Oliver, 1987) as well as terminations of PVCN neurons in the SOC (Thompson and Thompson, 1991b).

Functional implications

Our data demonstrate that planar neurons project to MOC neurons. Furthermore, the morphology of the synapses they form, with round vesicles and a prominent density, suggests that they excite MOC neurons (Uchizono, 1965; Bae et al., 1999; Paik et al., 2009). We thus propose that planar neurons are the intermediate stage of the MOC reflex, the limb that initiates the MOC neurons to respond to sound. The expected conduction velocity of planar neuron axons, which are myelinated and average 1.64 μm diameter, is 10 m/s (Sakai and Woody, 1988). Using our length measurement of 4.59 mm from CN to VNTB, we predict a travel time of 0.44 ms in mouse, and would be perhaps twice as long in guinea pig. A minimal response latency of 3–5 ms is reported for chopper units, the physiological correlate of planar neurons (Rhode and Smith, 1986; Blackburn and Sachs, 1989; Taberner and Liberman, 2005). Finally, using a similar length measurement from MOC soma back to the ipsilateral cochlea, an additional travel time of approximately 0.5 ms would be expected. Adding these three times produces a value consistent with the minimum response latency of MOC neurons recorded at the spiral ganglion, which is 5 – 7 ms (Brown, 1989).

The idea that planar neurons are the intermediate stage is also consistent with the narrow frequency tuning of chopper units (Rhode et al., 1983; Rhode and Smith, 1986; Palmer et al., 1996). Planar neuron dendrites are restricted to a narrow frequency-specific band in VCN (Doucet et al., 1999; Doucet and Ryugo, 1997), so they are expected to receive inputs from auditory nerve fibers tuned to a narrow range of characteristic frequencies. Narrowly tuned inputs would produce the narrow tuning of MOC neurons (Robertson and Gummer, 1985; Liberman and Brown, 1986; Brown, 1989). Overall, our data are consistent with the idea that planar multipolar neurons form the intermediate limb of the MOC reflex.

Acknowledgments

Grant sponsor: National Institutes of Health-NIDCD, grant number DC01089 (to M.C.B.)

We thank Dr. M. C. Liberman for reviewing a previous version of this manuscript, and Ms. Marie Drottar for technical assistance. Preliminary results of this study were presented in abstract form at the Association for Research in Otolaryngology Midwinter Meetings, February, 2010 and February, 2011.

LITERATURE CITED

Adams JC. Multipolar cells in the ventral cochlear nucleus project to the dorsal cochlear nucleus and the inferior colliculus. Neuroscience Letters. 1983; 37:205–208. [PubMed: 6888799]

Adams JC, Warr WB. Origins of axons in the cat's acoustic striae determined by injections of horseradish into severed tracts. J Comp Neurol. 1976; 170:107–122. [PubMed: 61976]

Aschoff A, Ostwald J. Distribution of cochlear efferents and olivo-collicular neurons in the brainstem of rat and guinea pig. Exp Brain Res. 1988; 71:241–251. [PubMed: 3169161]

Bae YC, Tatsuzo N, Ihn HJ, Choi MH, Yoshida A, Moritani M, Shiho H, Shigenaga Y. Distribution pattern of inhibitory and excitatory snapses in the dendritic tree of single masseter alpha-motoneurons in the cat. J Comp Neurol. 1999; 414:454–468. [PubMed: 10531539]

Benson TE, Brown MC. Ultrastructure of synaptic input to medial olivocochlear neurons. J Comp Neurol. 2006; 499:244–257. [PubMed: 16977616]

Blackburn CC, Sachs MB. Classification of unit types in the anteroventral cochlear nucleus: PST histograms and regularity analysis. J Neurophysiol. 1989; 62:1303–1329. [PubMed: 2600627]

Brown MC. Morphology and response properties of single olivocochlear fibers in the guinea pig. Hearing Res. 1989; 40:93–110.

Brown MC, Drottar M, Benson TE, Darrow KN. Commissural axons of the mouse cochlear nucleus. Assoc Res Otolaryngol Abstr In Press. 2012

Brown MC, de Venecia RK, Guinan JJ Jr. Responses of medial olivocochlear (MOC) neurons: Specifying the central pathways of the MOC reflex. Exp Brain Res. 2003; 153:491–498. [PubMed: 14557911]

Brown MC, Levine JL. Dendrites of medial olivocochlear (MOC) neurons in mouse. Neurosci. 2008; 154:147–159.

Campbell JP, Henson MM. Olivocochlear neurons in the brainstem of the mouse. Hearing Res. 1988; 35:271–274.

Cant NB. The fine structure of two types of stellate cells in the anterior division of the anteroventral cochlear nucleus of the cat. Neurosci. 1981; 6:2643–2655.

Caicedo A, Herbert H. Topography of descending projections from the inferior colliculus to auditory brainstem in the rat. J Comp Neurol. 1993; 328:377–392. [PubMed: 7680052]

Darrow KN, Maison SF, Liberman MC. Selective removal of lateral olivocochlear efferents increases vulnerability to acute acoustic injury. J Neurophysiol. 2007; 97:1775–1785. [PubMed: 17093118]

de Venecia RK, Liberman MC, Guinan JJ Jr, Brown MC. Medial olivocochlear reflex interneurons are located in the posteroventral cochlear nucleus. J Comp Neurol. 2005; 487:345–360. [PubMed: 15906311]

Doucet JR, Ross AT, Gillespie MB, Ryugo DK. Glycine immunoreactivity of multipolar neurons in the ventral cochlear nucleus which project to the dorsal cochlear nucleus. J Comp Neurol. 1999; 408:515–531. [PubMed: 10340502]

Doucet JR, Ryugo DK. Projections from the ventral cochlear nucleus to the dorsal cochlear nucleus in rats. J Comp Neurol. 1997; 385:245–264. [PubMed: 9268126]

Doucet JR, Ryugo DK. Axonal pathways to the lateral superior olive labeled with biotinylated dextran amine injections in the dorsal cochlear nucleus in rats. J Comp Neurol. 2003; 461:452–465. [PubMed: 12746862]

Doucet JR, Ryugo DK. Structural and functional classes of multipolar cells in the ventral cochlear nucleus. Anat Rec A. 2006; 288A:331–344.

Hackney CM, Osen KK, Kolston J. Anatomy of the cochlear nuclear complex of the guinea pig. Anat Embryol. 1990; 182:123–149. [PubMed: 2244686]

Helfert RH, Schwartz IR, Ryan AF. Ultrastructural characterization of gerbil olivocochlear neurons based on differential uptake of 3H-D-Aspartic acid and a wheatgerm agglutinin-horseradish peroxidase conjugate from the cochlea. J Neuroscience. 1988; 8:3111–3123.

Liberman MC, Brown MC. Physiology and anatomy of single olivocochlear neurons in the cat. Hearing Res. 1986; 24:17–36.

Liberman MC, Oliver ME. Morphometry of intracellularly labeled neurons of the auditory nerve: Correlations with functional properties. J Comp Neurol. 1984; 223:163–176. [PubMed: 6200517]

Mulders WHAM, Robertson D. Morphological relationships of peptidergic and noradrenergic nerve terminals to olivocochlear neurones in the rat. Hearing Res. 2000; 144:53–64.

Oertel D, Wright S, Cao X, Ferragamo M, Bal R. The multiple functions of T stellate/multipolar/chopper cells in the ventral cochlear nucleus. Hearing Res. 2011; 276:61–69.

Oliver DL. Projections to the inferior colliculus from the anteroventral cochlear nucleus in the cat: Possible substrates for binaural interaction. J Comp Neurol. 1987; 264:24–46. [PubMed: 2445792]

Ostapoff EM, Morest DK, Parham K. Spatial organization of the reciprocal connections betweem the cat dorsal and anteroventral cochlear nuclei. Hear Res. 1999; 130:75–93. [PubMed: 10320100]

Paik SK, Lee HJ, Choi MK, Cho YS, Park MJ, Moritani M, Yoshida A, Kim YS, Bae YC. Ultrastructural analysis of glutamate-, GABA-, and glycine-immunopositive boutons from supratrigeminal premotoneurons in the rat trigeminal motor nucleus. J Neurosci Res. 2009; 87:1115–1122. [PubMed: 19006082]

Palmer AR, Jiang D, Marshall DH. Responses of ventral cochlear nucleus onset and chopper units as a function of signal bandwidth. J Neurophysiol. 1996; 75:780–794. [PubMed: 8714652]

Rhode WS, Oertel D, Smith PH. Physiological response properties of cells labeled intracellularly with horseradish peroxidase in cat ventral cochlear nucleus. J Comp Neurol. 1983; 213:448–463. [PubMed: 6300200]

Rhode WS, Smith P. Encoding of timing and intensity in the ventral cochlear nucleus of the cat. J Neurophysiol. 1986; 56:261–286. [PubMed: 3760921]

Robertson D, Gummer M. Physiological and morphological characterization of efferent neurons in the guinea pig cochlea. Hearing Res. 1985; 20:63–77.

Ryugo, DK.; Fay, RR.; Popper, AN. Auditory and Vestibular Efferents. New York: Springer Science +Business Media, LLC; 2011. p. 359

Sakai J, Woody CD. Relationships between axonal diameter, soma size, and axonal conduction velocity of HRP-filled, pyramidal tract cells of awake cats. Brain Res. 1988; 460:1–7. [PubMed: 2464399]

Smith, PH.; Joris, PX.; Banks, MI.; Yin, TCT. Responses of cochlear nucleus cells and projections of their axons. In: Merchan, MA.; Juiz, JM.; Godfrey, DA.; Mugnaini, E., editors. The Mammalian Cochlear Nuclei: Organization and Function. New York: Plenum Press; 1993. p. 349-360.

Spangler KM, White JS, Warr WB. Electron microscopic features of axon terminals on olivocochlear neurons in the cat. Assoc Res Otolaryngol Abstr. 1986; 9:37–38.

Taberner AM, Liberman MC. Response properties of single auditory nerve fibers in the mouse. J Neurophysiol. 2005; 93:557–569. [PubMed: 15456804]

Thompson AM, Thompson GC. Posteroventral cochlear nucleus projections to olivocochlear neurons. J Comp Neurol. 1991a; 303:267–285. [PubMed: 2013640]

Thompson AM, Thompson GC. Projections from the posteroventral cochlear nucleus to the superior olivary complex in the guinea pig: Light and EM observations with the PHA-L method. J Comp Neurol. 1991b; 311:495–508. [PubMed: 1757599]

Uchizono K. Characteristics of excitatory and inhibitory synapses in the central nervous system of the cat. Nature. 1965; 207:642–643. [PubMed: 5883646]

Warr WB. Fiber degeneration following lesions in the posteroventral cochlear nucleus of the cat. Exp Neurol. 1969; 23:140–155. [PubMed: 5765002]

White JS. Fine structure of medial olivocochlear neurons in the rat. Soc Neurosci Abstr. 1984; 10:393.

Wickesberg RE, Oertel D. Delayed, frequency-specific inhibition in the cochlear nuclei of mice: A mechanism for monaural echo suppression. J Neurosci. 1990; 10(6):1762–1768. [PubMed: 1972392]

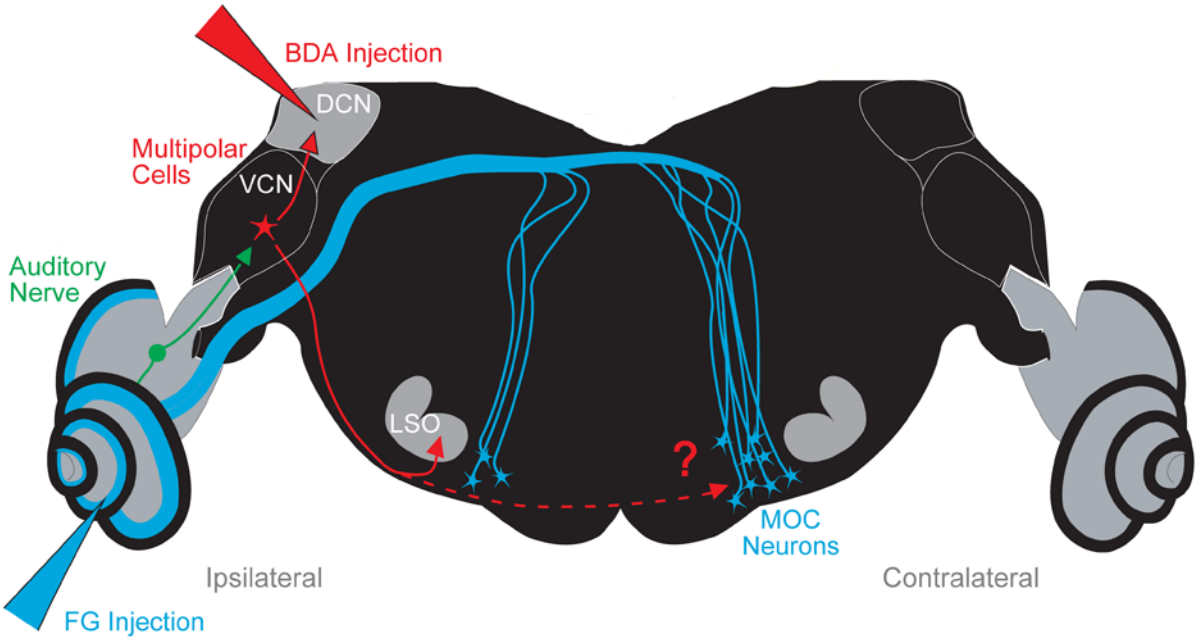

Figure 1.

Neural pathway of the medial olivocochlear (MOC) neurons projecting to the left cochlea (Ipsilateral side). Also shown are the stages of the reflex pathway leading to the MOC neurons: the auditory nerve fibers that project to the ventral cochlear nucleus (VCN), and the VCN multipolar cells that presumably project to MOC neurons. To test the hypothesis that multipolar cells project to MOC neurons, we labeled them via their collaterals using biotinylated dextran amine (BDA) injected into the dorsal cochlear nucleus (DCN). Multipolar cell axons were followed into the superior olivary complex (SOC), where many form branches to the lateral superior olive (LSO) on the ipsilateral side as reported previously (Doucet and Ryugo, 2003). Results of the present study show that they also form branches to the ventral nucleus of the trapezoid body (VNTB) on the contralateral side, the location of most MOC neurons in the mouse. In some experiments, a second injection of Fluorogold (FG) was made into the cochlea to retrogradely label MOC neurons.

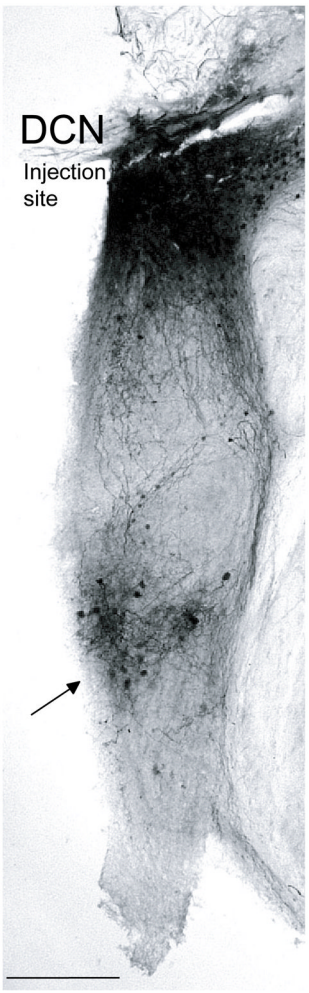

Figure 2.
Light micrograph of a transverse section containing the DCN injection site. More ventral is the band of labeling in the VCN (arrow) that contains labeled multipolar cells, their dendrites, and auditory nerve fibers. Scale bar = 250 μm.

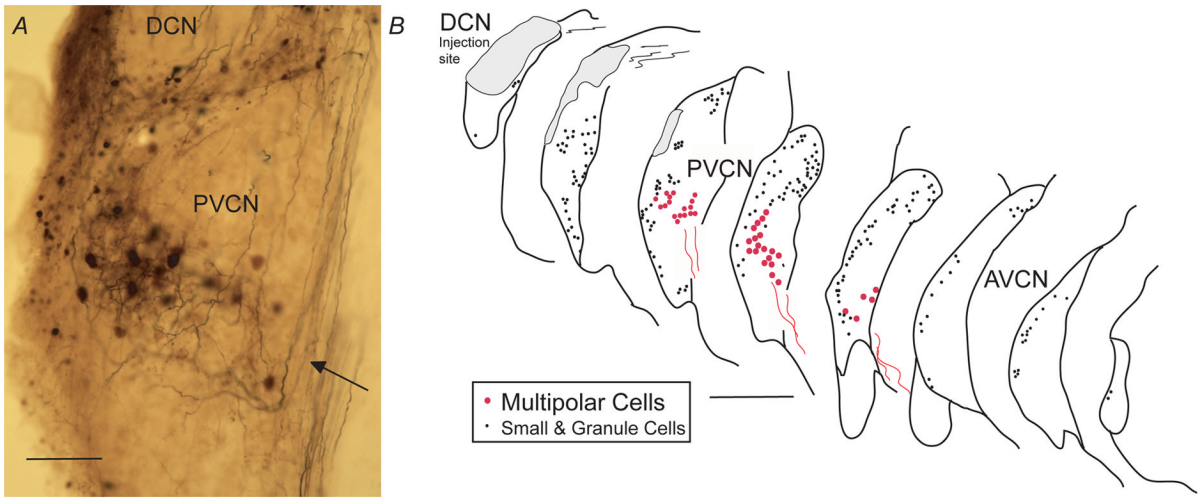

Figure 3.

A. Light micrograph showing the pattern of multipolar-cell labeling in a band (arrow) in the PVCN. Labeled processes are mainly branches of auditory nerve fibers. Smaller cells and granule cells are labeled at the lateral margin (left side of micrograph) and in the lamina dividing the PVCN from the DCN. Scale bar = 100 μm. **B.** Atlas drawings showing positions of multipolar cell (red circles) and small and granule cells (black dots). Labeled multipolar cell axons (red lines) project out of the nucleus in a ventromedial direction. Each panel of the atlas shows the labeled neurons in single 80-μm sections with half (every other one) of the sections omitted for clarity. Scale bar = 500 μm.

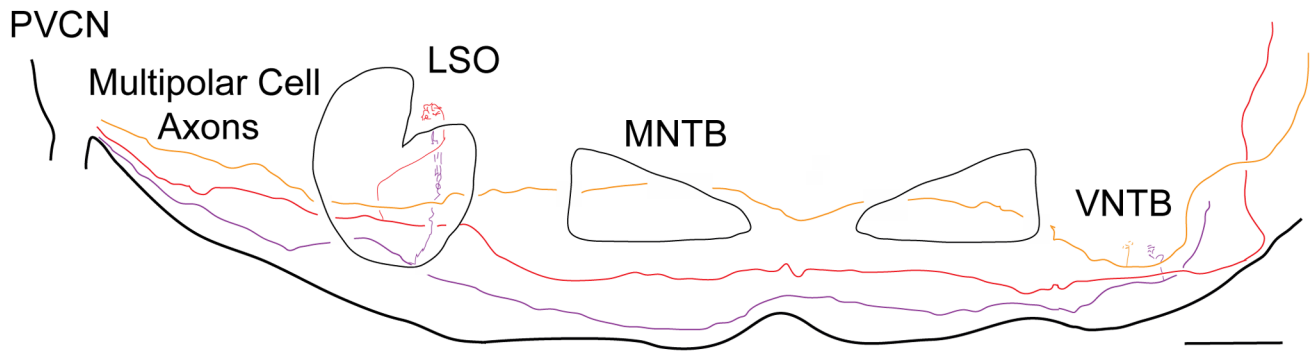

Figure 4.

Camera lucida drawing of presumed multipolar cell axons projecting from the PVCN through the SOC. The three axons illustrate branching to: 1) ipsilateral LSO (purple and red fibers), and 2) contralateral VNTB, (red and orange fibers). The branches to the LSO could not be completely reconstructed because of intermingling with other labeled branches that are not illustrated, but the branches to the VNTB were spatially separated and could be fully reconstructed. All axons continue on in the lateral lemniscus towards the inferior colliculus (not drawn). MNTB: medial nucleus of the trapezoid body. Scale bar = 500 μm.

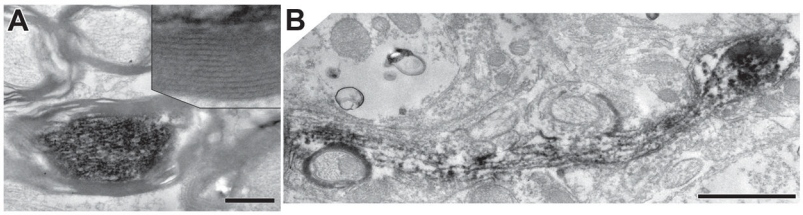

Figure 5.

A: Electron micrograph of a labeled axon from presumed multipolar cell axon in the trapezoid body near the contralateral VNTB, showing the axon's myelination and reaction product in the axoplasm. Scale bar = 0.5 μm. Inset: myelin lamellae at higher magnification. **B:** Micrograph of a labeled branch to contralateral VNTB showing reaction product in axoplasm but lack of myelination. The branch forms a swelling (right) but analysis of serial sections through this swelling failed to find a synapse. Scale bar = 1 μm.

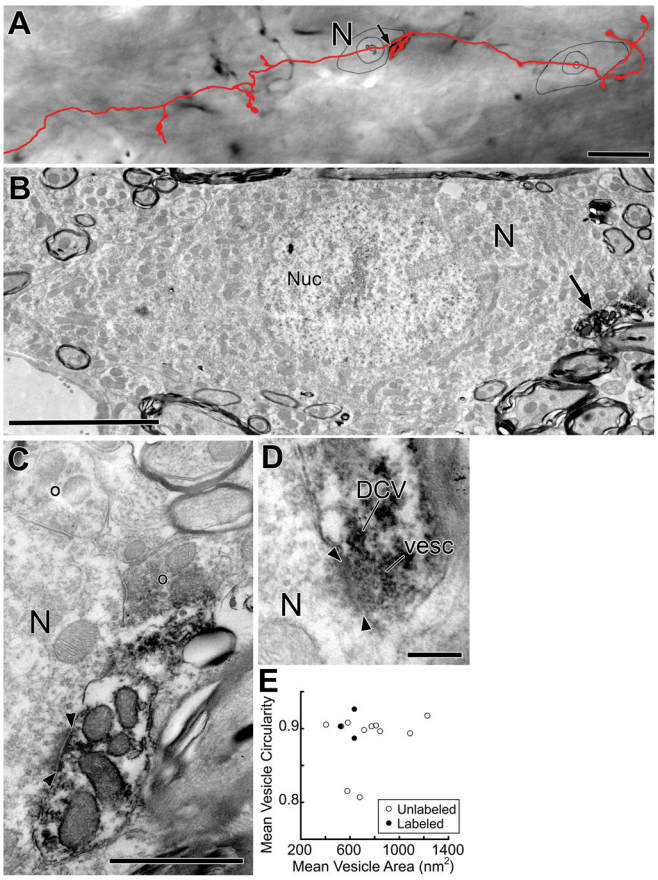

Figure 6.

Light and electron micrographs of a labeled branch in the contralateral VNTB. **A:** Light micrograph and reconstruction of a labeled branch (red). The branch has a large swelling that contacts (arrow) a neuron (N). Scale bar = 20 μm. **B:** Electron micrograph of the same neuron (N) in a section containing the nucleus (Nuc). The neuron is contacted (arrow) by the labeled swelling (note black reaction product), which forms a synapse (see C). Surrounding this neuron are numerous axons and small amounts of neuropil. Scale bar = 5 μm. **C, D:** High-magnification micrographs of different sections of the synapse (denoted by arrowheads) from the swelling. The labeled swelling contains synaptic vesicles and this one has a dense core vesicle (DCV, panel D). In the upper portion of C, two unlabeled terminals, denoted by open circles, are seen to form synapses onto the neuron (N). Scale bars = 1 μm for C, 0.2 μm for D. **E:** Mean vesicle circularity versus mean vesicle area (see Methods) from unlabeled and labeled synaptic terminals contacting this neuron. Terminals used for measurements were from the labeled branch (closed circles) or from unlabeled terminals (open circles) onto neuron N.

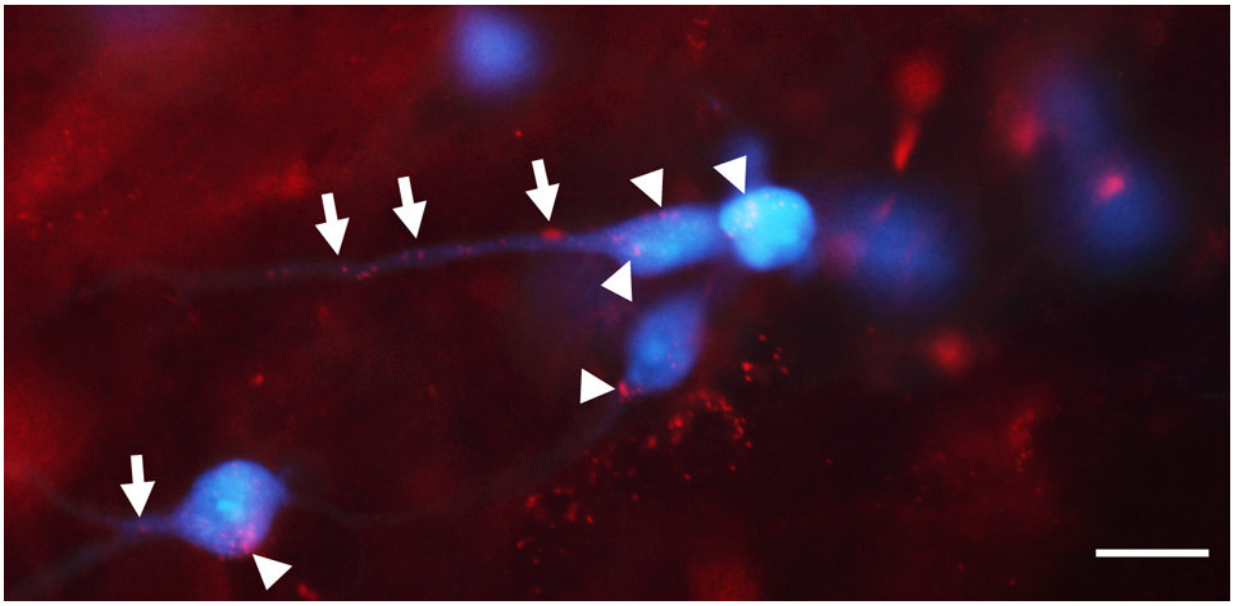

Figure 7.
Light micrograph of the contralateral VNTB showing boutons of presumed multipolar cells (red) that contact MOC neurons (blue) on their somata (arrowheads) and dendrites (arrows). In this double-injected case, fluorescently tagged DA (red) was injected into the DCN and Fluorogold (blue) was injected in the cochlea. Scale bar = 15 μm.

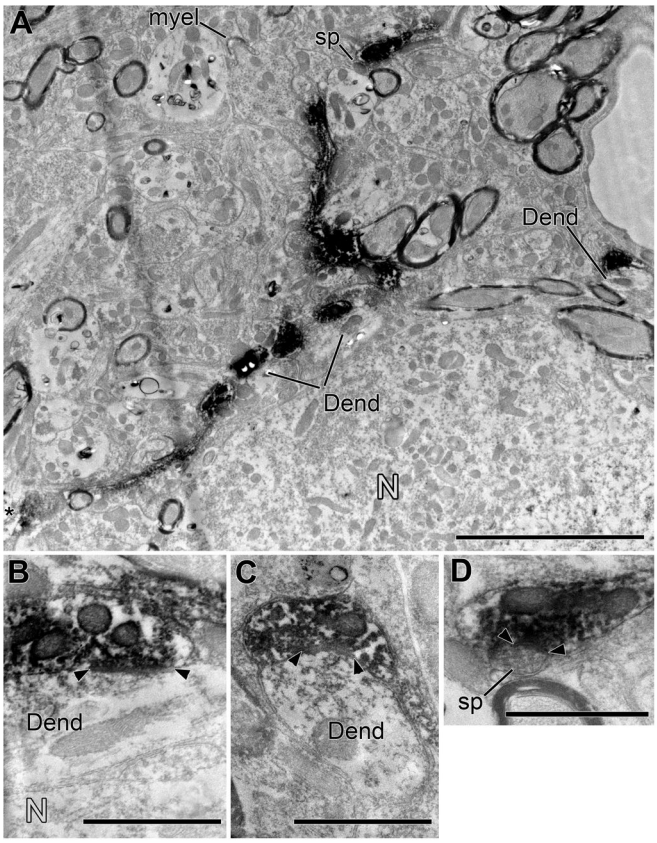

Figure 8.

Electron microscopy of a labeled branch from a different case than Figure 6. **A:** Low-magnification electron micrograph shows a labeled branch winding through the contralateral VNTB neuropil adjacent to a neuron (N). The neuron was not a postsynaptic target in our material, but nearby postsynaptic targets included two dendrites (Dend, one of them indicated in two segments in the center and confirmed to be contiguous in serial sections) and a spine (sp). In the neuropil, an axon of unknown origin forms a large ending as it loses its myelin (myel). Scale bar = 5 μm. **B–D:** Higher-magnifications of the synapses on dendrites (Dend) and a dendritic spine (sp). Panel B reveals a dendrite intervening between the labeled branch and the neuron. Scale bars = 1 μm.